




## Implications of the isobar-run results for the chiral magnetic effect in heavy-ion collisions

Dmitri E. Kharzeev <sup>1,2,\*</sup>, Jinfeng Liao <sup>3,†</sup> and Shuzhe Shi <sup>1,‡</sup>

<sup>1</sup>Center for Nuclear Theory, Department of Physics and Astronomy, Stony Brook University, Stony Brook, New York 11794-3800, USA

<sup>2</sup>Department of Physics, Brookhaven National Laboratory, Upton, New York 11973-5000, USA

<sup>3</sup>Physics Department and Center for Exploration of Energy and Matter, Indiana University, 2401 N Milo B. Sampson Lane, Bloomington, Indiana 47408, USA



(Received 18 May 2022; accepted 9 November 2022; published 28 November 2022)

The chiral magnetic effect (CME) is a macroscopic transport phenomenon induced by a quantum anomaly in the presence of chiral imbalance and an external magnetic field. Relativistic heavy ion collisions provide the unique opportunity to look for CME in a non-Abelian plasma, where the chiral imbalance is created by topological transitions similar to those occurring in the early universe. The isobar run at Relativistic Heavy Ion Collider was proposed as a way to separate the possible CME signal driven by magnetic field from the background. The first blind analysis results from this important experiment were recently released by the STAR Collaboration. Under the pre-defined assumption of identical background in RuRu and ZrZr, the results are inconsistent with the presence of CME, as well as with all existing theoretical models (whether including CME or not). However the observed difference of backgrounds must be taken into account before any physical conclusion is drawn. In this paper, we show that once the observed difference in hadron multiplicity and collective flow are quantitatively taken into account, the STAR results could be consistent with a finite CME signal contribution of about  $(6.8 \pm 2.6)\%$ .

DOI: [10.1103/PhysRevC.106.L051903](https://doi.org/10.1103/PhysRevC.106.L051903)

*Introduction.* The chiral magnetic effect (CME) is a macroscopic transport phenomenon induced by a quantum anomaly in chiral matter. In the presence of an external magnetic field  $\mathbf{B}$  and a chiral imbalance, the CME amounts to the generation of an electric current  $\mathbf{J}$  along  $\mathbf{B}$ :

$$\mathbf{J} = \sigma_5 \mathbf{B}, \quad (1)$$

where  $\sigma_5$  is the chiral magnetic conductivity that is proportional to the chiral chemical potential parametrizing the chirality imbalance between the left- and right-handed chiral fermions [1–3]. The CME has an impact on the physics of high-density QCD matter [1–6], condensed matter physics [7–11], astrophysics [12–14], cosmology [15–17], plasma physics [18–20], and quantum information [21,22]; for reviews, see, e.g., [23–31].

Relativistic heavy ion collisions provide a unique opportunity to create and study a quark-gluon plasma (QGP) at a temperature of over a trillion degrees. In QGP, the fluctuations of quark chirality imbalance are generated through the topological fluctuations of gluon fields. Moreover, the QGP produced in heavy ion collisions experiences an extremely strong magnetic field [2] created mostly by the fast-moving spectator protons. Thus the CME is expected to occur in the produced QGP [1], and may lead to a detectable signal in these

collisions [32]. The observation of CME in heavy ion collisions would establish the presence of topological fluctuations in a non-Abelian plasma, which represent a crucial ingredient of the baryon asymmetry generation in the early universe.

Extensive experimental efforts have been made by STAR, ALICE, and CMS Collaborations to look for CME in collisions at both the Relativistic Heavy Ion Collider (RHIC) and the Large Hadron Collider (LHC) [33–37]; see reviews [38–40]. The search has proved to be challenging due to a relatively small signal masked by a strong background contamination [32,41–44]; see, e.g., discussions in [38–40,45–47].

To disentangle the signal driven by magnetic field (in addition to topological fluctuations) and the background driven by the collective flow determined by the collision geometry, it has been proposed to perform a measurement of CME observables in RuRu and ZrZr isobar collisions [48,49]. The motivation for this measurement was that the similar size and shape of the colliding nuclei would lead to a nearly identical background, whereas the difference in electric charge of Ru and Zr nuclei would result in a difference in the created magnetic field, and thus in a difference in the observed CME signal.

In 2018 the STAR Collaboration performed the corresponding measurements at RHIC. A careful blind analysis was carried out subsequently [50], with the first set of data released in September 2021 [51]. STAR results are inconsistent with the “predefined” criteria for the CME, i.e., the criteria based on the assumption that the backgrounds in RuRu and ZrZr collisions are identical. Namely, the ratios of the CME observables measured in RuRu and ZrZr collisions are smaller than

\*dmitri.kharzeev@stonybrook.edu

†liaoji@indiana.edu

‡shuzhe.shi@stonybrook.edu

1, whereas a stronger magnetic field in RuRu system would apparently make this ratio bigger than 1 in the presence of CME. The problem with this result, however, is that if the CME is absent, the ratios of these observables would have to be *equal* to 1, and not be smaller than 1. Indeed, none of the theory models predicted the ratio smaller than 1, so this experimental result begs for an explanation.

The examination of STAR data [51] shows the key to understanding this puzzle is the observed difference between the gross properties of hadron production in RuRu and ZrZr collisions that stem from the difference in the shape and size of Ru and Zr nuclei. This *observed* difference in the multiplicity distributions and the collective flow invalidates the “predefined” criteria for the presence of CME, and clearly indicates the need for a post-blinding reanalysis of STAR data. Only after such an analysis is performed will one be able to draw conclusions about the presence or absence of CME in the data. In this Letter, we address this issue by combining insights from theoretical simulations based on the event-by-event anomalous-viscous fluid dynamics (EBE-AVFD) framework [52–56] with the analysis of STAR data. *Correlation observables.* In heavy ion collisions, the CME leads to a charge separation along the magnetic field which is approximately perpendicular to the reaction plane [57]. Such a charge separation can be measured via charge-dependent azimuthal correlations [32–34], with the most commonly used  $\Delta\gamma$  and  $\Delta\delta$  observables defined as

$$\Delta\gamma \equiv [\cos(\phi_1 + \phi_2 - 2\Psi_2)]_{\text{OS-SS}}, \quad (2)$$

$$\Delta\delta \equiv [\cos(\phi_1 - \phi_2)]_{\text{OS-SS}}. \quad (3)$$

Above,  $\phi_{1,2}$  are azimuthal angles of the charged hadron pairs while  $\Psi_2$  is the event-plane angle. The “OS – SS” means the difference between the opposite-sign hadron pairs (i.e., the pairs of hadrons with opposite electric charges) and same-sign pairs. Other observables have also been developed and used for experimental analysis [46,51], such as  $\Delta\gamma$  comparison between reaction and event plane [58,59],  $\Delta\gamma$  invariant mass dependence [60],  $R$  correlator [61], signed balance function [62], event-shape engineering [36,63], and others.

The CME signal induces the parity-odd harmonic in the azimuthal angle distribution of charged hadrons [1]:

$$\frac{dN_{\pm}}{d\phi} \sim 1 \pm 2a_1 \sin(\phi - \Psi_2) + \dots$$

Therefore it contributes to the above observables as  $\Delta\gamma_{cme} = +2a_1^2$  and  $\Delta\delta_{cme} = -2a_1^2$ , which are thus proportional to the square of the magnetic field strength.

The main challenge in the experimental search of CME is the background correlations that dominate the observables. The identified backgrounds are local charge conservation at hydrodynamic freeze-out and resonance decays. Their contributions to the observables scale approximately as  $\Delta\gamma_{bkg} \propto +\frac{v_2}{N_{ch}}$  and  $\Delta\delta_{bkg} \propto +\frac{1}{N_{ch}}$ , where  $N_{ch}$  is the charged particle multiplicity and  $v_2$  is the elliptic flow coefficient. One may also consider the observable  $\Delta\tilde{\gamma} \equiv \Delta\gamma/v_2$  for which  $\Delta\tilde{\gamma}_{bkg} \propto +\frac{1}{N_{ch}}$ . Such scaling behaviors were found to approximately hold in model simulations. For more detailed discussions on signals and backgrounds see, e.g., [46].

The isobar collision experiment in principle allows one to separate the signal and background contributions. In the idealized scenario, the two systems would be identical in their bulk properties (such as multiplicity and collective flow), which would result in the identical background contributions to the  $\Delta\gamma$  and  $\Delta\delta$  correlators. Therefore in the case of pure background, with no CME present, the measured isobar ratios would be  $\Delta\gamma^{\text{Ru}}/\Delta\gamma^{\text{Zr}} = 1$  and  $\Delta\delta^{\text{Ru}}/\Delta\delta^{\text{Zr}} = 1$ . The case of a finite CME contribution would imply  $\Delta\gamma^{\text{Ru}}/\Delta\gamma^{\text{Zr}} > 1$  and  $\Delta\delta^{\text{Ru}}/\Delta\delta^{\text{Zr}} < 1$ . These are the “predefined criteria” used in the STAR blind analysis [50,51]. However, as clearly shown by the STAR data, the bulk properties of hadrons produced in the two isobar systems are *not* identical. For example, in the same centrality class, the hadron multiplicities differ at a few percent level; this difference is extremely important in the search for the  $\approx 1\%$  CME effect. This situation requires a more careful isobar comparison with a proper baseline identification.

*Isobar multiplicity comparison.* As discussed above, the event multiplicity plays a key role in the background correlations and it is important to first examine the multiplicity difference between the two isobar pairs. While the Ru and Zr nuclei have an equal number of nucleons, the geometric distributions of protons and neutrons within these nuclei have a non-negligible difference [66–68]. This difference translates into the difference in the initial conditions (e.g., the participant and the binary collision densities), which in turn affects the subsequent bulk evolution and leads to the observed discrepancy in multiplicity.

First, we will show that by adopting suitable parameters (like charge radius, neutron skin, and harmonic deformation coefficients) for Ru and Zr nuclear distributions, one can reasonably reproduce the observed multiplicity difference. In Fig. 1 (upper panel), we show the ratio for the multiplicity distribution  $P(N_{ch})$  between RuRu and ZrZr from simulations with several choices for the nuclear parameters [51,64,65]. The STAR data are also shown for comparison, along with vertical bars indicating centrality class definition by STAR analysis. The simulation results compare well with data for the (20–50)% centrality class which will be the focus of our analysis. Considerable deviations occur in the very central and peripheral regions where fluctuations and uncertainties of both simulations and data become large. In Fig. 1 (lower panel) for the ratio of average multiplicity between RuRu and ZrZr in the same centrality class as defined by the STAR analysis, one sees nice agreement between simulation results and experimental data. With such multiplicity difference quantitatively accounted for, one can expect the simulations to provide useful and realistic baseline resulting from the background correlations. *Understanding the measured correlations.* Given the isobar multiplicity difference, a reasonable way to compare the correlators is to take into account the expected scaling behavior of background correlations by examining the following rescaled correlators:  $N_{ch} \times \Delta\gamma/v_2$  and  $N_{ch} \times \Delta\delta$ . Using STAR data from [51,69], we plot these re-scaled observables for RuRu and ZrZr in Fig. 2 (upper panels) as well as the RuRu/ZrZr ratios (lower panels).

Let us discuss the RuRu/ZrZr ratios shown in the lower panels of Fig. 2. If the background correlations were to

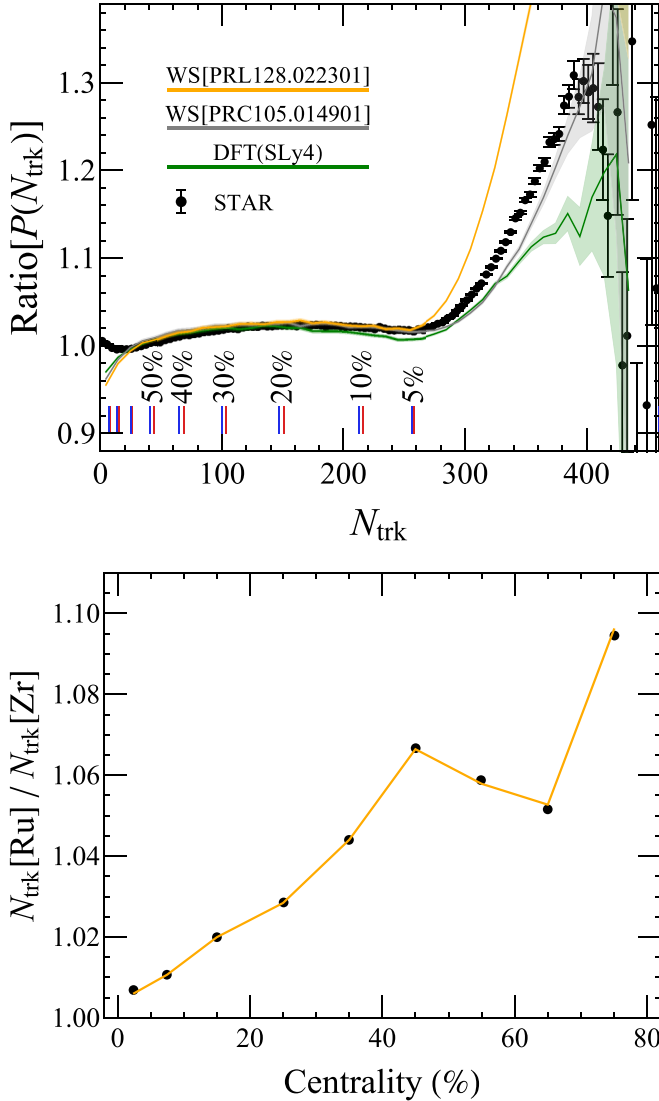


FIG. 1. The ratios of the multiplicity distribution  $P(N_{ch})$  (upper panel) and of the average multiplicity in the same centrality class measured in RuRu and ZrZr collisions as defined by the STAR analysis (lower panel). The orange, grey, and green curves are simulation results taking initial nucleon distributions in the colliding nuclei to be deformed [64] and spherical [51] Woods-Saxon distributions and density functional theory calculation [65], respectively. In the upper panel, red (blue) vertical bars indicate centrality class definition by STAR analysis for RuRu (ZrZr) collisions.

scale exactly as  $v_2/N_{ch}$ , then the pure-background baseline for both  $N_{ch} \times \Delta\gamma/v_2$  and  $N_{ch} \times \Delta\delta$  ratios would be unity. (As a caveat, the nonflow effect has the potential of shifting this ratio at about the 1% level and requires careful scrutiny [70].) A nonzero CME contribution on top of the baseline would then lead to  $R_\gamma \equiv [N_{ch} \times \Delta\gamma/v_2]_{\text{RuRu/ZrZr}} > 1$  and  $R_\delta \equiv [N_{ch} \times \Delta\delta]_{\text{RuRu/ZrZr}} < 1$ . As one can see from Fig. 2, the ratio for the scaled  $\gamma$  correlator is around unity for very central collisions and gradually increases to a value well above one towards the relatively more peripheral region.

This trend is consistent with a nonzero CME contribution that should increase with growing magnetic field strength

from central to peripheral collisions. On the other hand, the ratio for the scaled  $\delta$  correlator also increases from unity in very central collisions to be above unity in more peripheral collisions, while a nonzero CME contribution would have decreased this ratio to be below unity. This apparent “inconsistency” between the  $\gamma$  and  $\delta$  trends requires a closer scrutiny of the background behavior.

To resolve this issue, we have used our (20–50)% simulation events in the pure background case to verify the assumption about the  $1/N_{ch}$  background scaling. It turns out that the scaling is not exact and a non-negligible additional dependence on the average transverse momentum  $\langle p_T \rangle$  can be identified, especially in the  $\delta$  correlator. The physical origin of this effect is due to the initial fluctuations that could induce a spread of radial flow “push” and thus a spread of  $\langle p_T \rangle$  even for events with similar multiplicity. Stronger radial flow (i.e., larger  $\langle p_T \rangle$ ) would lead to a stronger angular collimation of correlated charged hadron pairs, and thus to the enhancement of background correlations [42].

To demonstrate the impact of this effect on the  $\delta$  and  $\gamma$  correlators, we bin the (20–50)% simulation events based on  $\langle p_T \rangle$  and compute the corresponding correlators in each bin. The results, plotted in Fig. 3, clearly show a linear increase of  $N_{ch} \times \Delta\delta$  with  $\langle p_T \rangle$ . The  $N_{ch} \times \Delta\gamma/v_2$ , on the other hand, appears to be relatively insensitive to the  $\langle p_T \rangle$ . We also note that hydrodynamic simulations performed in [71] and in our calculations demonstrate that the RuRu events have a larger  $\langle p_T \rangle$  than ZrZr events in the same centrality class.

Our findings suggest that while unity is a suitable baseline ratio of the  $N_{ch} \times \Delta\gamma/v_2$  correlator, flow-induced corrections need to be taken into account for the baseline ratio of  $N_{ch} \times \Delta\delta$ . Since the RuRu system has a larger multiplicity than ZrZr system in the same centrality class, the scaled  $\delta$  correlator would have a relative enhancement in the RuRu system due to a slightly larger radial flow “push.” To quantify this correction, we have evaluated the baseline ratio from pure background case to be 1.033 by using the (20–50)% AVFD simulation events for the isobar pairs. In short, our analysis of the baseline ratios can be summarized as  $R_\gamma^{\text{baseline}} = 1$  and  $R_\delta^{\text{baseline}} = 1.033$  for (20–50)% collisions, shown as blue lines in Fig. 2 (lower panels). Comparing with the corresponding STAR data,  $R_\gamma^{\text{STAR}} = 1.011 > R_\gamma^{\text{baseline}}$  and  $R_\delta^{\text{STAR}} = 1.028 < R_\delta^{\text{baseline}}$ , shown as red bands in Fig. 2 (lower panels), we conclude that both the scaled  $\gamma$  and  $\delta$  correlators are consistent with a nonzero CME contribution.

*Extracting CME signal fraction.* Given the indication of a nonzero CME signal from our analysis above, we now make an attempt to extract the CME signal fraction from both the  $\gamma$  and  $\delta$  correlators based on the available information for (20–50)% centrality from the STAR data as well as from the simulation results.

Let us first examine the  $\Delta\bar{\gamma}$  correlator. Assuming that the CME signal fraction is  $f_s$ , we split the correlator measured in RuRu collisions into a signal and background contributions as follows:

$$\Delta\bar{\gamma}_s^{\text{Ru}} = f_s \Delta\bar{\gamma}^{\text{Ru}}, \quad (4)$$

$$\Delta\bar{\gamma}_b^{\text{Ru}} = (1 - f_s) \Delta\bar{\gamma}^{\text{Ru}}, \quad (5)$$

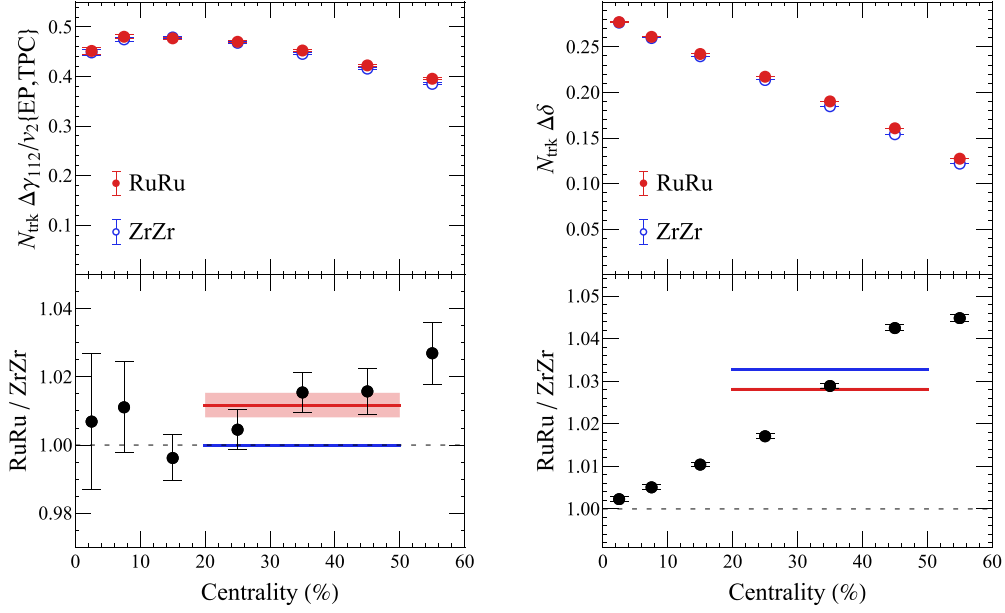


FIG. 2. Comparison between RuRu and ZrZr measurements for scaled correlators  $N_{ch} \times \Delta\gamma/v_2$  (left) and  $N_{ch} \times \Delta\delta$  (right), with the lower panels showing the RuRu to ZrZr ratios. The STAR data are taken from [51,69]. In the lower panels, the red shaded bands indicate measured values with error bars for (20–50)% while the blue lines indicate the baselines from the present simulation analysis.

where the subscripts  $s$  and  $b$  denote the signal and background components, respectively. Since the ZrZr collisions are expected to possess a weaker magnetic field, and thus relatively

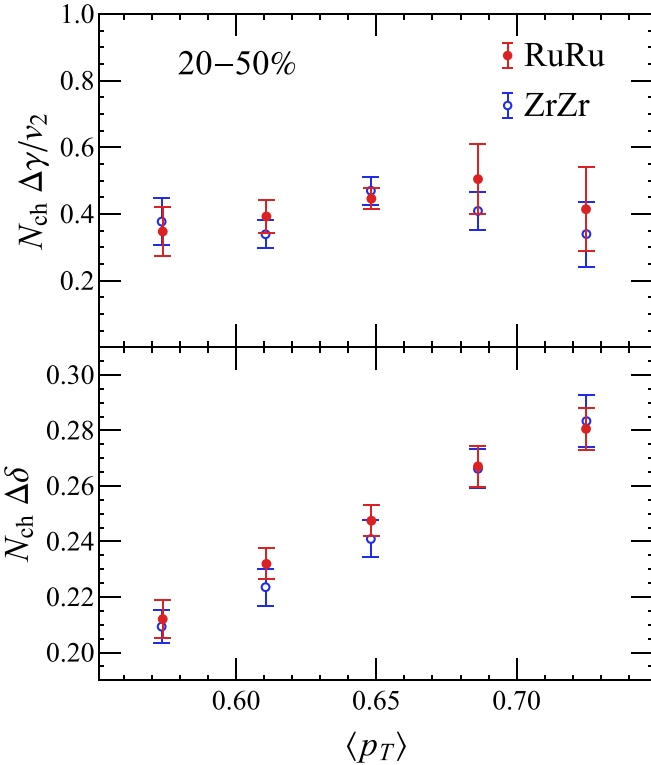


FIG. 3. The dependence of scaled  $\gamma$  (upper) and  $\delta$  (lower) correlators from pure background contributions on the average transverse momentum  $\langle p_T \rangle$  from simulations for (20–50)% centrality.

smaller signal and larger background, we then rescale these quantities from RuRu to ZrZr collisions as follows:

$$\Delta\bar{\gamma}_s^{\text{Zr}} = (1 - \lambda_s)\Delta\bar{\gamma}_s^{\text{Ru}} = (1 - \lambda_s)f_s\Delta\bar{\gamma}^{\text{Ru}}, \quad (6)$$

$$\Delta\bar{\gamma}_b^{\text{Zr}} = (1 + \lambda_b)\Delta\bar{\gamma}_b^{\text{Ru}} = (1 + \lambda_b)(1 - f_s)\Delta\bar{\gamma}^{\text{Ru}}. \quad (7)$$

Therefore, the total  $\Delta\bar{\gamma}$  correlator for ZrZr is:

$$\begin{aligned} \Delta\bar{\gamma}^{\text{Zr}} &= \Delta\bar{\gamma}^{\text{Ru}} \times [(1 - \lambda_s)f_s + (1 + \lambda_b)(1 - f_s)] \\ &= \Delta\bar{\gamma}^{\text{Ru}}[1 + \lambda_b - (\lambda_s + \lambda_b)f_s], \end{aligned} \quad (8)$$

which means the  $\Delta\bar{\gamma}$  ratio between the isobars is

$$R = \frac{\Delta\bar{\gamma}^{\text{Ru}}}{\Delta\bar{\gamma}^{\text{Zr}}} = \frac{1}{1 + \lambda_b - (\lambda_s + \lambda_b)f_s}. \quad (9)$$

Let us rewrite the ratio as  $R \equiv \frac{1}{1 + \lambda_R}$  (or equivalently  $\lambda_R = 1/R - 1$ ) and then we can express the  $f_s$  as

$$f_s = \frac{\lambda_b - \lambda_R}{\lambda_s + \lambda_b}. \quad (10)$$

Under the naïve assumption of identical backgrounds in RuRu and ZrZr systems, as used in the STAR predefined criteria, the pure background case would correspond to  $\lambda_b = \lambda_R = f_s = 0$ , while a nonzero signal would correspond to  $\lambda_b = 0$ ,  $\lambda_R < 0$  and  $f_s > 0$ . This assumption is, however, invalidated by the data, as already discussed above.

The estimates based on experimental data and simulations suggest instead the following values: (a)  $R \simeq 0.9641 \pm 0.0037$  or  $\lambda_R \simeq +(0.0372 \pm 0.0040)$  directly from measurements; (b)  $\lambda_b$ , dominated by the multiplicity difference, is estimated according to the ratio of  $\langle N^{-1} \rangle$  and  $\lambda_b \simeq +0.0508$ ; (c) The isobar signal ratio is dictated by the magnetic fields, for which the ratio is determined from simulations to be  $\lambda_s \simeq +(0.15 \pm 0.05)$  [66]. See Supplemental Material [72] for details of how these values are obtained or estimated.



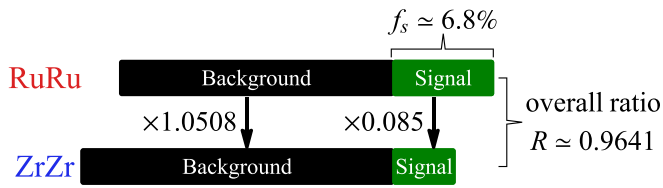


FIG. 4. An illustration of the comparison between isobar systems for the measured  $\bar{\gamma}$  correlators, with signal and background components indicated as black and green bars. The lengths of the bars are not plotted in exact proportion and the signal parts are graphically magnified for visibility. See text for details.

Putting these inputs together, one arrives at the following estimate for the CME signal fraction in the measured  $\Delta\bar{\gamma}$  correlator:

$$f_s \simeq +(0.068 \pm 0.026) = (6.8 \pm 2.6)\%. \quad (11)$$

We note that this value is consistent with the isobar analysis results from the event-plane/spectator-plane contrast method [51]. To make the outcome of this analysis more transparent, we illustrate it in Fig. 4.

*Summary.* To summarize, we have combined the insights from theoretical simulations with the analysis of STAR experimental data to understand the implications of isobar collisions for the chiral magnetic effect. First, we have shown that the measured multiplicity difference between the RuRu and ZrZr systems, which plays a key role for establishing the background baseline, can be successfully described by simulations with suitable initial nuclear structure inputs. Furthermore, we have identified the radial flow “push” as an important contributor to background correlations, in addition to the multiplicity and elliptic flow. Quantitatively accounting for these two effects on the backgrounds has allowed us a calibration of the appropriate baselines for both the scaled  $\gamma$  and  $\delta$  correlators. Compared with the experimental data, we conclude that the correlation measurements could be consistent with a finite CME signal contribution, estimated at a level of about  $(6.8 \pm 2.6)\%$  fraction, as illustrated in Fig. 4. Such a fraction is obtained by assuming that the non-CME background of  $\Delta\bar{\gamma}$  is inversely proportional to multiplicity. There is however nonflow effect [70] that could make nontrivial contributions to background ratio, the influence of which

clearly deserves future investigations (see Supplemental Material [72] for more discussions).

Let us discuss possible future measurements that can further help to establish or rule out the presence of CME signal in heavy ion collisions. Given that the radial flow push is found to impact the calibration of backgrounds, it would be very useful to measure and compare the average transverse momentum of charged particles between the isobar systems. Another useful approach for the isobar comparison is to apply identical event selection criteria for multiplicity,  $v_2$ , and  $\langle p_T \rangle$  and then compare the subset of isobar events that are ensured to have identical background correlations [52,66]. Both the participant-plane/spectator-plane contrast method [58,59] and the event-shape engineering approach [73] have the potential of maximizing the signal/background contrast, extracting the signal fraction and allowing a verification of expected signal scaling between isobar pairs. Beyond the  $\gamma$  and  $\delta$  correlators, it would be interesting to understand the background scaling and their implications for the interpretation of isobar comparison in, e.g., the  $R$  correlator [74] as well as the signed balance function [62]. Finally, it is of great importance to achieve a coherent understanding of both isobar and AuAu systems [75]. Recent STAR measurements in AuAu collisions based on the participant-plane/spectator-plane contrast method, while suffering from a limited statistics, do suggest a nonzero CME fraction of  $(6.3\text{--}14.7)\%$  [76]. Future high precision measurements based on the anticipated large sample of AuAu events together with the ongoing post-blinding analysis of the extensive isobar data set will hopefully allow us to improve the statistical significance of these results and to make a conclusive statement on the presence or absence of CME in heavy ion collisions.

*Acknowledgments.* We thank H. Caines, Y. Hu, H. Huang, R. Lacey, S. Pratt, A. Tang, P. Tribedy, S. Voloshin, F. Wang, G. Wang, and Z. Xu for useful discussions and communications. This work is partly supported by the U.S. Department of Energy, Office of Science, Office of Nuclear Physics, within the framework of the Beam Energy Scan Theory (BEST) Topical Collaboration. D.K. and S.S. also acknowledge support by the U.S. Department of Energy, Office of Science, Office of Nuclear Physics, Grants No. DE-FG88ER40388 and No. DE-SC0012704. J.L. also acknowledges support by the NSF Grant No. PHY-2209183.

- [1] D. Kharzeev, Parity violation in hot QCD: Why it can happen, and how to look for it, *Phys. Lett. B* **633**, 260 (2006).
- [2] D. E. Kharzeev, L. D. McLerran, and H. J. Warringa, The Effects of topological charge change in heavy ion collisions: “Event by event  $\mathcal{P}$  and  $\mathcal{CP}$  violation”, *Nucl. Phys. A* **803**, 227 (2008).
- [3] K. Fukushima, D. E. Kharzeev, and H. J. Warringa, Chiral magnetic effect, *Phys. Rev. D* **78**, 074033 (2008).
- [4] D. Kharzeev, R. D. Pisarski, and M. H. G. Tytgat, Possibility of Spontaneous Parity Violation in Hot QCD, *Phys. Rev. Lett.* **81**, 512 (1998).
- [5] D. Kharzeev, A. Krasnitz, and R. Venugopalan, Anomalous chirality fluctuations in the initial stage of heavy ion collisions and parity odd bubbles, *Phys. Lett. B* **545**, 298 (2002).
- [6] D. Kharzeev and A. Zhitnitsky, Charge separation induced by  $\mathcal{P}$ -odd bubbles in QCD matter, *Nucl. Phys. A* **797**, 67 (2007).
- [7] D. T. Son and B. Z. Spivak, Chiral anomaly and classical negative magnetoresistance of Weyl metals, *Phys. Rev. B* **88**, 104412 (2013).
- [8] A. A. Zyuzin and A. A. Burkov, Topological response in Weyl semimetals and the chiral anomaly, *Phys. Rev. B* **86**, 115133 (2012).
- [9] G. Basar, D. E. Kharzeev, and H.-U. Yee, Triangle anomaly in Weyl semimetals, *Phys. Rev. B* **89**, 035142 (2014).
- [10] Q. Li, D. E. Kharzeev, C. Zhang, Y. Huang, I. Pletikosic, A. V. Fedorov, R. D. Zhong, J. A. Schneeloch, G. D. Gu, and T. Valla, Observation of the chiral magnetic effect in ZrTe<sub>5</sub>, *Nat. Phys.* **12**, 550 (2016).

- [11] X. Huang *et al.*, Observation of the Chiral-Anomaly-Induced Negative Magnetoresistance in 3D Weyl Semimetal TaAs, *Phys. Rev. X* **5**, 031023 (2015).
- [12] D. Grabowska, D. B. Kaplan, and S. Reddy, Role of the electron mass in damping chiral plasma instability in supernovae and neutron stars, *Phys. Rev. D* **91**, 085035 (2015).
- [13] Y. Masada, K. Kotake, T. Takiwaki, and N. Yamamoto, Chiral magnetohydrodynamic turbulence in core-collapse supernovae, *Phys. Rev. D* **98**, 083018 (2018).
- [14] N. Yamamoto, Chiral transport of neutrinos in supernovae: Neutrino-induced fluid helicity and helical plasma instability, *Phys. Rev. D* **93**, 065017 (2016).
- [15] H. Tashiro, T. Vachaspati, and A. Vilenkin, Chiral effects and cosmic magnetic fields, *Phys. Rev. D* **86**, 105033 (2012).
- [16] A. Vilenkin and D. A. Leahy, Parity nonconservation and the origin of cosmic magnetic fields, *Astrophys. J.* **254**, 77 (1982).
- [17] A. Vilenkin, Equilibrium parity-violating current in a magnetic field, *Phys. Rev. D* **22**, 3080 (1980).
- [18] Y. Akamatsu and N. Yamamoto, Chiral Plasma Instabilities, *Phys. Rev. Lett.* **111**, 052002 (2013).
- [19] Y. Hirono, D. E. Kharzeev, and Y. Yin, Quantized Chiral Magnetic Current from Reconnections of Magnetic Flux, *Phys. Rev. Lett.* **117**, 172301 (2016).
- [20] E. V. Gorbar, I. A. Shovkovy, S. Vilchinskii, I. Rudenok, A. Boyarsky, and O. Ruchayskiy, Anomalous Maxwell equations for inhomogeneous chiral plasma, *Phys. Rev. D* **93**, 105028 (2016).
- [21] D. E. Kharzeev and Q. Li, The chiral qubit: quantum computing with chiral anomaly, [arXiv:1903.07133](https://arxiv.org/abs/1903.07133)
- [22] V. Shevchenko, Quantum measurements and chiral magnetic effect, *Nucl. Phys. B* **870**, 1 (2013).
- [23] D. E. Kharzeev and J. Liao, Chiral magnetic effect reveals the topology of gauge fields in heavy-ion collisions, *Nat. Rev. Phys.* **3**, 55 (2021).
- [24] D. E. Kharzeev, J. Liao, S. A. Voloshin, and G. Wang, Chiral magnetic and vortical effects in high-energy nuclear collisions—A status report, *Prog. Part. Nucl. Phys.* **88**, 1 (2016).
- [25] D. E. Kharzeev, The chiral magnetic effect and anomaly-induced transport, *Prog. Part. Nucl. Phys.* **75**, 133 (2014).
- [26] K. Fukushima, Extreme matter in electromagnetic fields and rotation, *Prog. Part. Nucl. Phys.* **107**, 167 (2019).
- [27] K. Hattori and X.-G. Huang, Novel quantum phenomena induced by strong magnetic fields in heavy-ion collisions, *Nucl. Sci. Technol.* **28**, 26 (2017).
- [28] J.-H. Gao, G.-L. Ma, S. Pu, and Q. Wang, Recent developments in chiral and spin polarization effects in heavy-ion collisions, *Nucl. Sci. Technol.* **31**, 90 (2020).
- [29] A. A. Burkov, Chiral anomaly and transport in Weyl metals, *J. Phys.: Condens. Matter* **27**, 113201 (2015).
- [30] N. P. Armitage, E. J. Mele, and A. Vishwanath, Weyl and Dirac semimetals in three dimensional solids, *Rev. Mod. Phys.* **90**, 015001 (2018).
- [31] I. A. Shovkovy, Anomalous plasma: chiral magnetic effect and all that, [arXiv:2111.11416](https://arxiv.org/abs/2111.11416).
- [32] S. A. Voloshin, Parity violation in hot QCD: How to detect it, *Phys. Rev. C* **70**, 057901 (2004).
- [33] B. I. Abelev *et al.* (STAR Collaboration), Azimuthal Charged-Particle Correlations and Possible Local Strong Parity Violation, *Phys. Rev. Lett.* **103**, 251601 (2009).
- [34] B. I. Abelev *et al.* (STAR Collaboration), Observation of charge-dependent azimuthal correlations and possible local strong parity violation in heavy ion collisions, *Phys. Rev. C* **81**, 054908 (2010).
- [35] S. Acharya *et al.* (ALICE Collaboration), Constraining the chiral magnetic effect with charge-dependent azimuthal correlations in Pb-Pb collisions at  $\sqrt{s_{NN}} = 2.76$  and 5.02 TeV, *J. High Energy Phys.* **09** (2020) 160.
- [36] S. Acharya *et al.* (ALICE Collaboration), Constraining the magnitude of the chiral magnetic effect with event shape engineering in Pb-Pb collisions at  $\sqrt{s_{NN}} = 2.76$  TeV, *Phys. Lett. B* **777**, 151 (2018).
- [37] V. Khachatryan *et al.* (CMS Collaboration), Observation of Charge-Dependent Azimuthal Correlations in  $p$ -Pb Collisions and Its Implication for the Search for the Chiral Magnetic Effect, *Phys. Rev. Lett.* **118**, 122301 (2017).
- [38] J. Zhao and F. Wang, Experimental searches for the chiral magnetic effect in heavy-ion collisions, *Prog. Part. Nucl. Phys.* **107**, 200 (2019).
- [39] W. Li and G. Wang, Chiral magnetic effects in nuclear collisions, *Annu. Rev. Nucl. Part. Sci.* **70**, 293 (2020).
- [40] A. Bzdak, S. Esumi, V. Koch, J. Liao, M. Stephanov, and N. Xu, Mapping the phases of quantum chromodynamics with Beam Energy Scan, *Phys. Rep.* **853**, 1 (2020).
- [41] F. Wang, Effects of cluster particle correlations on local parity violation observables, *Phys. Rev. C* **81**, 064902 (2010).
- [42] S. Pratt, Alternative contributions to the angular correlations observed at RHIC associated with parity fluctuations, [arXiv:1002.1758](https://arxiv.org/abs/1002.1758).
- [43] A. Bzdak, V. Koch, and J. Liao, Remarks on possible local parity violation in heavy ion collisions, *Phys. Rev. C* **81**, 031901(R) (2010).
- [44] A. Bzdak, V. Koch, and J. Liao, Azimuthal correlations from transverse momentum conservation and possible local parity violation, *Phys. Rev. C* **83**, 014905 (2011).
- [45] A. Bzdak, V. Koch, and J. Liao, Charge-dependent correlations in relativistic heavy Ion collisions and the chiral magnetic effect, in *Strongly Interacting Matter in Magnetic Fields*, Lecture Notes in Physics Vol. 871 (Springer, Berlin, 2013), p. 503.
- [46] S. Choudhury *et al.*, Investigation of experimental observables in search of the chiral magnetic effect in heavy-ion collisions in the STAR experiment, *Chin. Phys. C* **46**, 014101 (2022).
- [47] P. Christakoglou, S. Qiu, and J. Staa, Systematic study of the chiral magnetic effect with the AVFD model at LHC energies, *Eur. Phys. J. C* **81**, 717 (2021).
- [48] S. A. Voloshin, Testing the Chiral Magnetic Effect with Central  $U + U$  collisions, *Phys. Rev. Lett.* **105**, 172301 (2010).
- [49] V. Koch, S. Schlichting, V. Skokov, P. Sorensen, J. Thomas, S. Voloshin, G. Wang, and H.-U. Yee, Status of the chiral magnetic effect and collisions of isobars, *Chin. Phys. C* **41**, 072001 (2017).
- [50] J. Adam *et al.* (STAR Collaboration), Methods for a blind analysis of isobar data collected by the STAR collaboration, *Nucl. Sci. Technol.* **32**, 48 (2021).
- [51] M. Abdallah *et al.* (STAR Collaboration), Search for the chiral magnetic effect with isobar collisions at  $\sqrt{s_{NN}}=200$  GeV by the STAR Collaboration at the BNL Relativistic Heavy Ion Collider, *Phys. Rev. C* **105**, 014901 (2022).
- [52] S. Shi, H. Zhang, D. Hou, and J. Liao, Signatures of Chiral Magnetic Effect in the Collisions of Isobars, *Phys. Rev. Lett.* **125**, 242301 (2020).

- [53] S. Shi, Y. Jiang, E. Lilleskov, and J. Liao, Anomalous chiral transport in heavy ion collisions from anomalous-viscous fluid dynamics, *Ann. Phys.* **394**, 50 (2018).
- [54] Y. Jiang, S. Shi, Y. Yin, and J. Liao, Quantifying the chiral magnetic effect from anomalous-viscous fluid dynamics, *Chin. Phys. C* **42**, 011001 (2018).
- [55] X. An *et al.*, The BEST framework for the search for the QCD critical point and the chiral magnetic effect, *Nucl. Phys. A* **1017**, 122343 (2022).
- [56] C. Shen, Z. Qiu, H. Song, J. Bernhard, S. Bass, and U. Heinz, The iEBE-VISHNU code package for relativistic heavy-ion collisions, *Comput. Phys. Commun.* **199**, 61 (2016).
- [57] J. Błoczyński, X.-G. Huang, X. Zhang, and J. Liao, Azimuthally fluctuating magnetic field and its impacts on observables in heavy-ion collisions, *Phys. Lett. B* **718**, 1529 (2013).
- [58] Hao-jie Xu, J. Zhao, X. Wang, H. Li, Z.-W. Lin, C. Shen, and F. Wang, Varying the chiral magnetic effect relative to flow in a single nucleus-nucleus collision, *Chin. Phys. C* **42**, 084103 (2018).
- [59] S. A. Voloshin, Estimate of the signal from the chiral magnetic effect in heavy-ion collisions from measurements relative to the participant and spectator flow planes, *Phys. Rev. C* **98**, 054911 (2018).
- [60] J. Zhao, H. Li, and F. Wang, Isolating the chiral magnetic effect from backgrounds by pair invariant mass, *Eur. Phys. J. C* **79**, 168 (2019).
- [61] N. Magdy, S. Shi, J. Liao, N. Ajitanand, and R. A. Lacey, New correlator to detect and characterize the chiral magnetic effect, *Phys. Rev. C* **97**, 061901(R) (2018).
- [62] A. H. Tang, Probe chiral magnetic effect with signed balance function, *Chin. Phys. C* **44**, 054101 (2020).
- [63] F. Wen, J. Bryon, L. Wen, and G. Wang, Event-shape-engineering study of charge separation in heavy-ion collisions, *Chin. Phys. C* **42**, 014001 (2018).
- [64] C. Zhang and J. Jia, Evidence of Quadrupole and Octupole Deformations in  $^{96}\text{Zr} + ^{96}\text{Zr}$  and  $^{96}\text{Ru} + ^{96}\text{Ru}$  Collisions at Ultrarelativistic Energies, *Phys. Rev. Lett.* **128**, 022301 (2022).
- [65] Hao-jie Xu, H. Li, X. Wang, C. Shen, and F. Wang, Determine the neutron skin type by relativistic isobaric collisions, *Phys. Lett. B* **819**, 136453 (2021).
- [66] S. Shi, H. Zhang, D. Hou, and J. Liao, Chiral magnetic effect in isobaric collisions from anomalous-viscous fluid dynamics (AVFD), *Nucl. Phys. A* **982**, 539 (2019).
- [67] H.-J. Xu, X. Wang, H. Li, J. Zhao, Z.-W. Lin, C. Shen, and F. Wang, Importance of Isobar Density Distributions on the Chiral Magnetic Effect Search, *Phys. Rev. Lett.* **121**, 022301 (2018).
- [68] J. Hammelmann, A. Soto-Ontoso, M. Alvioli, H. Elfner, and M. Strikman, Influence of the neutron-skin effect on nuclear isobar collisions at energies available at the BNL Relativistic Heavy Ion Collider, *Phys. Rev. C* **101**, 061901(R) (2020).
- [69] M. S. Abdallah *et al.* (STAR Collaboration), Search for the chiral magnetic effect with isobar collisions at  $\sqrt{s_{NN}} = 200$  GeV by the STAR Collaboration at the BNL Relativistic Heavy Ion Collider, HEPData (collection) (2022), doi: 10.17182/hepdata.115993.
- [70] Y. Feng, J. Zhao, H. Li, Hao-jie Xu, and F. Wang, Two- and three-particle nonflow contributions to the chiral magnetic effect measurement by spectator and participant planes in relativistic heavy ion collisions, *Phys. Rev. C* **105**, 024913 (2022).
- [71] G. Nijs and W. van der Schee, Inferring nuclear structure from heavy isobar collisions using Trajectum, [arXiv:2112.13771](https://arxiv.org/abs/2112.13771).
- [72] See Supplemental Material at <http://link.aps.org/supplemental/10.1103/PhysRevC.106.L051903> for technical details on the simulations and analysis that have been used to obtain the results reported in the main Letter.
- [73] R. Milton, G. Wang, M. Sergeeva, S. Shi, J. Liao, and H. Z. Huang, Utilization of event shape in search of the chiral magnetic effect in heavy-ion collisions, *Phys. Rev. C* **104**, 064906 (2021).
- [74] R. A. Lacey, N. Magdy, P. Parfenov, and A. Taranenko, Scaling properties of background- and chiral-magnetically-driven charge separation in heavy ion collisions at  $\sqrt{s_{NN}} = 200$  GeV, [arXiv:2203.10029](https://arxiv.org/abs/2203.10029).
- [75] Y. Feng, Y. Lin, J. Zhao, and F. Wang, Revisit the chiral magnetic effect expectation in isobaric collisions at the relativistic heavy ion collider, *Phys. Lett. B* **820**, 136549 (2021).
- [76] M. Abdallah *et al.* (STAR Collaboration), Search for the Chiral Magnetic Effect via Charge-Dependent Azimuthal Correlations Relative to Spectator and Participant Planes in Au+Au Collisions at  $\sqrt{s_{NN}} = 200$  GeV, *Phys. Rev. Lett.* **128**, 092301 (2022).